Absolute densities of N and excited N2 in a N2 plasma

Absolute densities of N and excited N_2 in a N_2 plasma

Sumit Agarwal
Department of Chemical Engineering, University of California, Santa Barbara, California 93106-5080

Bram Hoex and M. C. M. van de Sanden
Department of Applied Physics, Eindhoven University of Technology, P.O. Box 513, 5600 MB, Eindhoven, The Netherlands

Dimitrios Maroudas
Department of Chemical Engineering, University of Massachusetts, Amherst, MA 01003-3110

Eray S. Aydil[a)]
Department of Chemical Engineering, University of California, Santa Barbara, California 93106-5080

(Received 8 July 2003; accepted 7 October 2003)

Atomic N and excited N_2 (N_2^*) play important roles in plasma-assisted synthesis of nitride materials, such as GaN. Absolute densities of N and N_2^* were measured at the substrate plane in an inductively coupled N_2 plasma in the pressure range of 10 to 200 mTorr using modulated-beam line-of-sight threshold ionization mass spectrometry. The density of N increased with increasing pressure from 2.9×10^{18} to 1.8×10^{19} m^{-3}, while the density of N_2^* was in the range of 9.7×10^{17} to 2.4×10^{18} m^{-3}, with a maximum at 50 mTorr. Based on the appearance potential of N_2^* at ~12 eV, we identify this excited molecule as long-lived N_2 ($A^3\Sigma_u^+$) metastable. © *2003 American Institute of Physics.* [DOI: 10.1063/1.1630843]

Nitrogen plasmas are used extensively in the low-temperature deposition of materials such as Si_3N_4,[1] C_3N_4,[2] and as the nitriding source in plasma-assisted molecular beam epitaxy of GaN.[3,4] Nitrogen plasmas contain atomic N, as well as electronically[5,6] and vibrationally excited N_2 that carry several electron volts of energy above the ground state. Any or all of these highly reactive species can affect the surface and, thus, the deposition chemistry. Several studies in the deposition of GaN using N_2 plasmas have revealed that the properties of the deposited thin films depend on the relative flux of N and excited N_2 (N_2^*) to the surface during growth.[7–9] Specifically, N_2^* is thought to be more desirable for GaN growth since it facilitates higher film growth rates at lower substrate temperatures with significantly improved electrical properties in comparison to growth with a predominantly atomic N flux.[7,8] Thus, there is a need to simultaneously characterize the N and N_2^* fluxes impinging on the substrate to determine the role of these precursors during deposition. In this letter, we report the use of modulated-beam line-of-sight threshold ionization mass spectrometry (LOS-TIMS) to measure the absolute densities of N and N_2^* in an N_2 plasma. Although TIMS has been used to measure N atom densities,[10,11] N_2^* measurements have not been reported previously.

In mass spectrometry, electron impact ionization of a radical and its parent molecule can result in the same daughter ion. For example, N^+ ions can be formed by both direct ionization of N radicals, ($N+e\rightarrow N^+ +2e$ with a threshold energy of 14.5 eV) and through dissociative ionization of N_2 molecules, ($N_2+e\rightarrow N^+ +N+2e$ with a threshold energy of 24.3 eV). The difference in the thresholds for direct and dissociative ionization enables the distinction of the quadrupole mass spectrometer (QMS) signal due to the radical species (N) from the signal due to its parent molecule (N_2) in the electron energy range between 14.5 and 24.3 eV. This principle for radical detection is referred to as TIMS. Using a similar principle, N_2^* can be differentiated from the ground state N_2 since the threshold for the parent ionization of N_2^* is lower than that for the ground state N_2. However, it is not possible to determine the identity of the excited species uniquely, that is, it is not possible to determine whether the excited species are vibrationally or electronically excited states of N_2.

The experiments were conducted in an inductively coupled plasma reactor, in which the plasma is excited using a planar coil powered at 13.56 MHz.[12] The power absorbed by the plasma and N_2 flow rate were kept constant at 750 W and 50 std. cm^3/min, respectively, while the gas pressure was varied from 10 to 200 mTorr. A QMS coupled with an in-line ''Bessel Box''-type ion-energy analyzer (Hiden PSM-2) was placed in LOS with the sampling orifice in a three-stage differentially pumped chamber.[13] The gas-phase species impinging on the substrate plane from the plasma were sampled through a 1 mm aperture on the substrate platen. A chopper was used to modulate the beam sampled from the plasma to separate the ions created from the species directly entering the QMS ionizer (beam component) from the ions created from species already present as background in the differentially pumped chamber (background component). The beam component is proportional to the concentration of the species of interest in the plasma chamber; it is obtained by taking the difference between ion counts measured with the chopper in the open (beam+background) and closed (background) positions.

Figure 1 shows the QMS signal for N^+ as a function of

a)Author to whom correspondence should be addressed; electronic mail: aydil@engineering.ucsb.edu

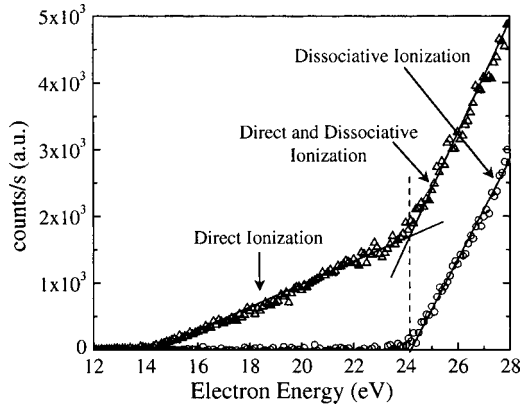

FIG. 1. QMS signal ($m/e=14$) for N^+ in counts/s as a function of electron energy with the chopper in the open (△) and closed (○) positions. The pressure in the plasma chamber was 50 mTorr.

the electron energy with the chopper in the open and closed positions. Since the electron-impact ionization cross sections are linear, with electron energy up to a few electron volts above the threshold, the threshold for ionization of N to form N^+ can be determined from the electron-energy intercept of a linear fit to the QMS signal in the direct ionization region with the chopper in the open position. This threshold is 14.5 eV, as would be expected for ionization of ground state N atoms. Similarly, the dissociative ionization threshold of N_2 to form N^+ is apparent at 24.3 eV from the data obtained with the chopper in the open and closed positions.

The QMS signal for N_2^+ ions as a function of electron energy is shown in Fig. 2. The threshold for the direct ionization of N_2 to form N_2^+ is at 15.6 eV, corresponding to transitions from the ground vibrational level of the ground electronic state ($X^1\Sigma_g^+$) of N_2 to the ground vibrational level of the ground electronic state of N_2^+ ($X^2\Sigma_g^+$). However, Fig. 2 shows that the direct ionization threshold is shifted to ~12 eV, 3.6 eV below the direct ionization threshold for the ground state N_2, indicating the presence of N_2^*. The QMS signal due to N_2^* with the chopper open is significantly higher than that with the chopper closed, indicating that the plasma is the source of N_2^*. The presence of some N_2^* signal in the background is due to N_2^* produced by the QMS ionizer filament. Taking into account the time of flight of the neutral species in the molecular beam from the sampling aperture to

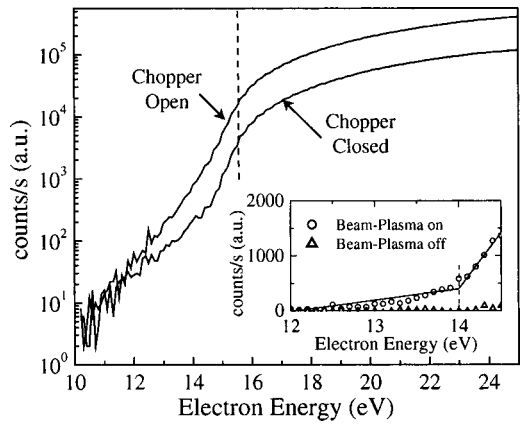

FIG. 2. QMS signal ($m/e=28$) for N_2^+ in counts/s corresponding to the data shown in Fig. 1.

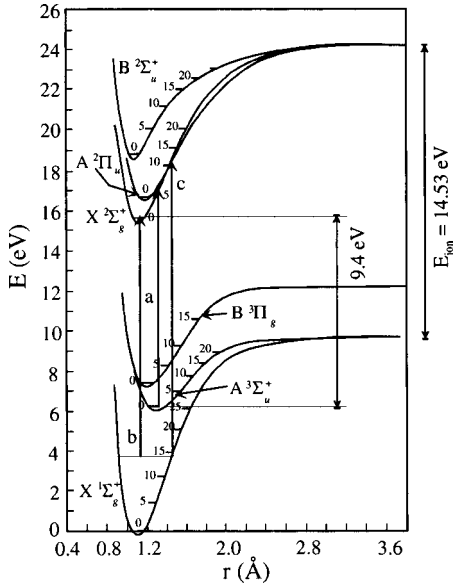

FIG. 3. Simplified potential energy curves for different electronic states of N_2 and N_2^+. The vertical arrows indicate the possible FC transitions during ionization and the numbers indicate the vibrational levels.

the QMS ionizer, the only candidates for the N_2^* detected in these experiments are N_2 in the lowest lying electronically excited $A^3\Sigma_u^+$ state (6.2 eV above ground level, with a radiative lifetime >2.0 s),[14] or vibrationally excited N_2 (up to the 27th vibrational level) in the $X^1\Sigma_g^+$ state (Fig. 3). All other electronic states of N_2 have a much shorter lifetime than the time of flight to the QMS ionizer.[15]

The identity of the N_2^* can be determined by considering various Franck–Condon (FC) transitions from the relevant N_2 to N_2^+ electronic states shown in Fig. 3. The ground vibrational level of the $A^3\Sigma_u^+$ state has a larger mean separation distance (r_e) compared to the $X^2\Sigma_g^+$ state of N_2^+ (15.6 eV above the $X^1\Sigma_g^+$ state, Fig. 3). Thus, a FC transition from the ground vibrational level of the $A^3\Sigma_u^+$ state to the ground vibrational level of the $X^2\Sigma_g^+$ state is improbable, as there is no overlap of the wave functions of these states. For a ground vibrational level, the wave function is a Gaussian centered at r_e, and the wave functions for the higher vibrational levels peak at the classical turning points of the potential energy curves. Thus, the observed ionization threshold could correspond to a transition from the center of the ground vibrational level of the $A^3\Sigma_u^+$ state to the classical turning point of a higher vibrational level of the $X^2\Sigma_g^+$ state or the $A^2\Pi_u$ state (e.g., transition "a" in Fig. 3). Such a transition would require ~11 eV, much closer to the observed threshold. The other possibility for the N_2^+ appearing at ~12 eV could be due to the presence of vibrationally excited states within the $X^1\Sigma_g^+$ electronic state.

In order to observe an ionization threshold of ~12 eV, the FC transition would have to be from approximately the 14th vibrational level of the ground $X^1\Sigma_g^+$ state to the ground vibrational level of the $X^2\Sigma_g^+$ state (transition "b" in Fig. 3). However, such a transition would correspond to a low FC overlap since the wave functions of vibrationally excited states peak at the classical turning points.

A transition from the turning points of the vibrationally excited $X^1\Sigma_g^+$ states to the turning points of vibrationally

excited $X\,^2\Sigma_g^+$ ionic state is likely, but will have a much higher threshold (14–15 eV), as shown by the vertical line "c" in Fig. 3. Indeed, a careful examination of the data in this region shows a knee in the QMS signal at ~14 eV. This cannot be due to the spread in the energy distribution of the electron beam [full width at half-maximum ~0.5 eV] which could shift the 15.6 eV threshold to lower energies. This knee is obvious in the inset shown in Fig. 2 and only in the signal with the plasma on. Thus, based on the potential energy diagram of the N_2 and N_2^+ electronic states, we conclude that the most likely candidate for the N_2^* species appearing at 12 eV is the ground and/or vibrationally excited $A\,^3\Sigma_u^+$ state, and the most likely candidate for N_2^* species appearing at 14 eV is the vibrationally excited $X\,^1\Sigma_g^+$ state.

The beam components of the QMS ion count rates shown in Figs. 1 and 2 for N and N_2^*, respectively, have to be calibrated to obtain absolute densities. We have used the calibration procedure described previously.[13,16,17] The absolute density of X (X=N or N_2^*), n_X^{on}, was calibrated with the signal from the parent ionization of a reference gas (Y) with known partial pressure and with an m/e value equal to or close to that of the species of interest, using the expression

$$\frac{n_X^{\text{on}}}{n_Y^{\text{off}}} = \left(\frac{S_{\text{beam}}^{X\to X^+}}{S_{\text{beam}}^{Y\to Y^+}}\right)\cdot\left(\frac{\sigma^{Y\to Y^+}}{\sigma^{X\to X^+}}\right), \tag{1}$$

where, $S_{\text{beam}}^{X\to X^+}$ and $S_{\text{beam}}^{Y\to Y^+}$ are the beam components of the QMS ion count rates for species X (with plasma on) and the reference species Y (with plasma off), respectively. n_Y^{off} can be calculated from known pressure and temperature (298 K) of species Y (Y=CH_4 for N, N_2, for N_2^*) in the plasma chamber with the discharge turned off. The relevant cross sections in Eq. (1), $\sigma^{X\to X^+}$ and $\sigma^{Y\to Y^+}$, are available from the literature.[18–21] The ionization cross section used for calculating N_2^* density was for ionization from the $A\,^3\Sigma_u^+$ state. Only the data up to 14 eV were used to calculate the $A\,^3\Sigma_u^+$ state density. There are no reliable ionization cross sections for the vibrationally excited $X\,^1\Sigma_g^+$ state, and we did not calculate their absolute densities. The absolute densities for N and N_2^* ($A\,^3\Sigma_u^+$) are shown in Fig. 4 as a function of the pressure in the plasma chamber. Figure 4 shows that the density of N increases with increasing pressure from 2.9×10^{18} to 1.8×10^{19} m^{-3}. The density of N_2^* is almost one order of magnitude lower (9.7×10^{17} to 2.4×10^{18} m^{-3}) except in a narrow range (~50 mTorr), in which the N_2^* density exhibits a maximum. Initially, the N_2^* density increases with increasing pressure up to 50 mTorr as more N_2 can be excited by electrons. At its maximum value, the N_2^* density is comparable to that of N at the same pressure. However, at high pressures, N_2^* decreases rapidly because collisional quenching with other N_2 molecules becomes the dominant de-excitation process. In contrast, N atom loss through N–N gas-phase recombination requires three-body collisions, which do not begin to compete with loss by diffusion to the chamber walls until higher pressures. Since diffusion losses decrease with increasing pressure, N atom density increases over the pressure range studied. In growth of GaN and other nitride materials, this difference in loss mechanisms and the resulting behavior of N_2^* and N densities with pressure can be exploited to maximize the flux of the nitrogen precursor beneficial for the growth process.

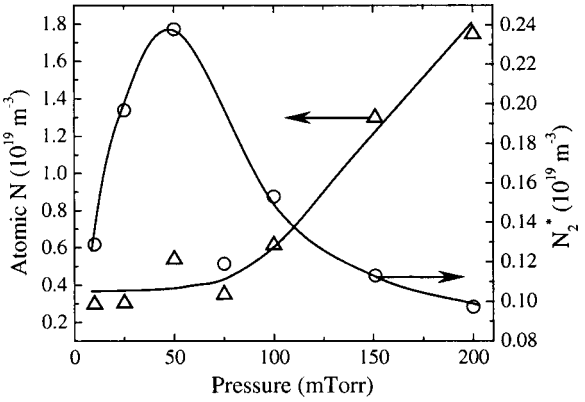

FIG. 4. Absolute N (△) and N_2^* (○) densities in the plasma as a function of pressure.

This work has been supported by the NSF/DoE Partnership for Basic Plasma Science and Engineering (Award No. ECS-0078711).

[1] B. F. Hanyaloglu and E. S. Aydil, J. Vac. Sci. Technol. A **16**, 2794 (1998).
[2] M. C. Polo, R. Aguiar, P. Serra, L. Cleries, M. Varela, and J. Esteve, Appl. Surf. Sci. **96–98**, 870 (1996).
[3] D. A. Neumayer and J. G. Ekerdt, Chem. Mater. **8**, 9 (1996).
[4] N. Newman, J. Cryst. Growth **178**, 102 (1997).
[5] V. Guerra, P. A. Sa, and J. Loureiro, J. Phys. D **34**, 1745 (2001).
[6] G. J. H. Brussaard, E. Aldea, M. C. M. van de Sanden, G. Dinescu, and D. C. Schram, Chem. Phys. Lett. **290**, 379 (1998).
[7] A. J. Ptak, M. R. Millecchia, T. H. Myers, K. S. Ziemer, and C. D. Stinespring, Appl. Phys. Lett. **74**, 3836 (1999).
[8] T. H. Myers, M. R. Millecchia, A. J. Ptak, K. S. Ziemer, and C. D. Stinespring, J. Vac. Sci. Technol. B **17**, 1654 (1999).
[9] S. H. Cho, H. Okumura, and K. Akimoto, Appl. Phys. Lett. **76**, 3861 (2000).
[10] H. Singh, J. W. Coburn, and D. B. Graves, J. Appl. Phys. **88**, 3748 (2000).
[11] D. Douai, J. Berndt, and J. Winter, Plasma Sources Sci. Technol. **11**, 60 (2002).
[12] S. Agarwal, A. Takano, M. C. M. van de Sanden, D. Maroudas, and E. S. Aydil, J. Chem. Phys. **117**, 10805 (2002).
[13] S. Agarwal, G. W. W. Quax, M. C. M. van de Sanden, D. Maroudas, and E. S. Aydil (unpublished).
[14] L. G. Piper, J. Chem. Phys. **99**, 3174 (1993).
[15] H. J. Werner, J. Kalcher, and E. A. Reinsch, J. Chem. Phys. **81**, 2420 (1984).
[16] H. Singh, J. W. Coburn, and D. B. Graves, J. Vac. Sci. Technol. A **17**, 2447 (1999).
[17] H. Singh, J. W. Coburn, and D. B. Graves, J. Vac. Sci. Technol. A **18**, 299 (2000).
[18] E. Brook, M. F. A. Harrison, and A. C. H. Smith, J. Phys. B **11**, 3115 (1978).
[19] R. S. Freund, R. C. Wetzel, and R. J. Shul, Phys. Rev. A **41**, 5861 (1990).
[20] H. C. Straub, P. Renault, B. G. Lindsay, K. A. Smith, and R. F. Stebbings, Phys. Rev. A **54**, 2146 (1996).
[21] C. C. Tian and C. R. Vidal, J. Phys. B **31**, 895 (1998).